Journal of Visualized Experiments
Focused Ion Beam Lithography to Etch Nano-architectures into Microelectrodes
--Manuscript Draft--

Article Type:	Invited Methods Article - JoVE Produced Video
Manuscript Number:	JoVE60004R2
Full Title:	Focused Ion Beam Lithography to Etch Nano-architectures into Microelectrodes
Keywords:	Focused ion beam lithography, intracortical microelectrodes, nano-architecture, electrophysiology, neuroinflammation, biocompatibility
Corresponding Author:	Evon S Ereifej US Department of Veterans Affairs Ann Arbor, Michigan UNITED STATES
Corresponding Author's Institution:	US Department of Veterans Affairs
Corresponding Author E-Mail:	eereifej@gmail.com
Order of Authors:	Evon S Ereifej
	Shreya Mahajan
	Jonah A Sharkins
	Allen H. Hunter
	Amir Avishai
Additional Information:	
Question	Response
Please indicate whether this article will be Standard Access or Open Access.	Standard Access (US$2,400)
Please indicate the **city, state/province, and country** where this article will be **filmed**. Please do not use abbreviations.	Ann Arbor, Michigan, USA

1   **TITLE:**
2   Focused Ion Beam Lithography to Etch Nano-architectures into Microelectrodes
3
4   **AUTHORS & AFFILIATIONS:**
5   Shreya Mahajan[1], Jonah A. Sharkins[2,4], Allen H. Hunter[5], Amir Avishai[6], Evon S. Ereifej[2,3,4]
6
7   [1]Department of Electrical Engineering and Computer Science, University of Michigan, Ann Arbor,
8   MI, USA
9   [2]Veteran Affairs Ann Arbor Healthcare System, Ann Arbor, MI 48105, USA
10   [3]Department of Neurology, School of Medicine, University of Michigan, Ann Arbor, MI, USA
11   [4]Department of Biomedical Engineering, University of Michigan, Ann Arbor, MI, USA
12   [5]Michigan Center for Materials Characterization, University of Michigan, Ann Arbor, MI, USA
13   [6]Carl Zeiss SMT, Inc., Pleasanton, CA, USA
14
15   Corresponding Author:
16   Evon S. Ereifej   (eereifej@aptcenter.org)
17
18   Email Addresses of Co-authors:
19   Shreya Mahajan   (shreyama@umich.edu)
20   Jonah A. Sharkins   (sharkins@umich.edu)
21   Allen Hunter   (ahhunter@umich.edu)
22   Amir Avishai   (amir.avishai@zeiss.com)
23
24   **KEYWORDS:**
25   Focused ion beam lithography, intracortical microelectrodes, nano-architecture,
26   electrophysiology, neuroinflammation, biocompatibility
27
28   **SUMMARY:**
29   We have shown that the etching of nano-architecture into intracortical microelectrode devices
30   may reduce the inflammatory response and has the potential to improve electrophysiological
31   recordings. The methods described herein outline an approach to etch nano-architectures into
32   the surface of non-functional and functional single shank silicon intracortical microelectrodes.
33
34   **LONG ABSTRACT:**
35   With advances in electronics and fabrication technology, intracortical microelectrodes have
36   undergone substantial improvements enabling the production of sophisticated microelectrodes
37   with greater resolution and expanded capabilities. The progress in fabrication technology has
38   supported the development of biomimetic electrodes, which aim to seamlessly integrate into the
39   brain parenchyma, reduce the neuroinflammatory response observed after electrode insertion
40   and improve the quality and longevity of electrophysiological recordings. Here we describe a
41   protocol to employ a biomimetic approach recently classified as nano-architecture. The use of
42   focused ion beam lithography (FIB) was utilized in this protocol to etch specific nano-architecture
43   features into the surface of non-functional and functional single shank intracortical
44   microelectrodes. Etching nano-architectures into the electrode surface indicated possible

45   improvements of biocompatibility and functionality of the implanted device. One of the benefits
46   of using FIB is the ability to etch on manufactured devices, as opposed to during the fabrication
47   of the device, facilitating boundless possibilities to modify numerous medical devices post-
48   manufacturing. The protocol presented herein can be optimized for various material types, nano-
49   architecture features, and types of devices. Augmenting the surface of implanted medical devices
50   can improve the device performance and integration into the tissue.
51
52   **INTRODUCTION:**
53   Intracortical Microelectrodes (IME) are invasive electrodes which provide a means of direct
54   interfacing between external devices and the neuronal populations inside the cerebral cortex[1,2].
55   This technology is an invaluable tool for recording neural action potentials to improve scientists'
56   ability to explore neuronal function, advance understanding of neurological diseases and develop
57   potential therapies. Intracortical microelectrode, used as a part of Brain Machine Interface (BMI)
58   systems, enables recording of action potentials from an individual or small groups of neurons to
59   detect motor intentions that can be used to produce functional outputs[3]. In fact, BMI systems
60   have successfully been used for prosthetic and therapeutic purposes, such as acquired
61   sensorimotor rhythm control to operate a computer cursor in patients with amyotrophic lateral
62   sclerosis (ALS)[4] and spinal cord injuries[5] and restoring the movement in people suffering from
63   chronic tetraplegia[6].
64
65   Unfortunately, IMEs often fail to record consistently over time due to several failure modes that
66   include mechanical, biological and material factors[7,8]. The neuroinflammatory response
67   occurring after the electrode implantation is thought to be a considerable challenge contributing
68   to electrode failure[9-14]. The neuroinflammatory response is initiated during the initial insertion
69   of the IME which severs the blood brain barrier, damages the local brain parenchyma and
70   disrupts glial and neuronal networks[15,16]. This acute response is characterized by the activation
71   of glial cells (microglia/macrophages and astrocytes), which release pro-inflammatory and
72   neurotoxic molecules around the implant site[17-20]. The chronic activation of glial cells results in a
73   foreign body reaction characterized by the formation of a glial scar isolating the electrode from
74   healthy brain tissue[7,9,12,13,17,21,22]. Ultimately, hindering the electrode's ability to record neuronal
75   action potentials, due to the physical barrier between the electrode and the neurons and the
76   degeneration and death of neurons[23-25].
77
78   The early failure of intracortical microelectrodes has brought about considerable research in the
79   development of next generation electrodes, with emphasis on biomimetic strategies[26-30]. Of
80   particular interest to the protocol described here, is the use of nano-architecture as a class of
81   biomimetic surface alterations for IMEs[31]. It has been established that surfaces mimicking the
82   architecture of the natural in vivo environment have an improved biocompatible response[32-36].
83   Thus, the hypothesis compelling this protocol is that the discontinuity between the rough
84   architecture of the brain tissue and smooth architecture of the intracortical microelectrodes may
85   contribute to the neuroinflammatory and chronic foreign body response to implanted IMEs (for
86   a full review refer to Kim et al.[31]). We have previously shown that the utilization of nano-
87   architecture features similar to the brain's extracellular matrix architecture reduces astrocyte
88   inflammatory markers from cells cultured on nano-architectured substrates, compared to flat

89 control surfaces in both in vitro and ex vivo models of neuroinflammation[37,38]. Furthermore, we
90 have shown the application of focused ion beam (FIB) lithography to etch nano-architectures
91 directly onto silicon probes resulted in significantly increased neuronal viability and lower
92 expression of pro-inflammatory genes from animals implanted with the nano-architecture
93 probes compared to the smooth control group[26]. Therefore, the purpose of the protocol
94 presented here is to describe the use of FIB lithography to etch nano-architectures on
95 manufactured intracortical microelectrode devices. This protocol was designed to etch nano-
96 architecture sized features into silicon surfaces of intracortical microelectrode shanks utilizing
97 both automated and manual processes. These methods are uncomplicated, reproducible, and
98 can certainly be optimized for various device materials and desired feature sizes.
99
100 **PROTOCOL:**
101
102 NOTE: Do the following steps while wearing the proper personal protective equipment, such as
103 a lab coat and gloves.
104
105 **1. Mounting non-functional silicon probe for focused ion beam (FIB) lithography**
106
107 NOTE: For the complete procedure describing the fabrication of the SOI wafer with the 1,000
108 probes, please refer to Ereifej et al.[39].
109
110 1.1 Isolate a strip of 2-3 silicon probes from the silicon on insulator (SOI) wafer containing 1,000
111 probes. Do not make strips containing more than three silicon probes. This may increase the
112 chances for loose mounting and may cause misalignment resulting in the FIB to etch incorrectly.
113
114 NOTE: Strips/probes not firmly sitting on the aluminum stub can cause two complications: 1)
115 when the stage moves to work on the next section, there will be vibrations and the milling will
116 not be accurate until the probe settles and 2) it can cause a high variation and be out of the focus
117 plane.
118
119 1.1.1 While wearing gloves, use fine forceps to put pressure around the probes to break off a
120 small section containing two to three probes.
121
122 1.2 Carefully clean the silicon probe of all dust and debris prior to FIB etching. Prepare a 6 well
123 polystyrene plate by pipetting 3 mL/well of 95% ethanol into three wells.
124
125 1.2.1 Carefully pick up the cut strip of silicon probes using fine tip or vacuum forceps and place it
126 into cell strainer. Place only one strip of silicon probes per strainer to prevent breaking the
127 probes. Place the strainer containing the silicon probes strip into the first well containing 95%
128 ethanol for cleaning. Keep the strainer in the first well for 5 min.
129
130 1.2.2 Move the strainer containing the silicon probes from the first well and place it into the
131 second well containing 95% ethanol for another 5 min. Repeat once more in the third well.
132

133 1.2.3 Place the strainer containing the cleaned silicon probes onto a polytetrafluoroethylene
134 plate to air dry. Do this step in a sterile hood to avoid contamination from dust.

136 1.3 Place the air-dried strip of silicon probes in a sealed container for transport to the SEM-FIB.
137 Wrap the strainer containing the air-dried samples with a plastic or aluminum foil wrap for
138 transport and/or storage to maintain cleaning.

140 1.4 Use fine tipped or vacuum forceps to carefully pick up the clean strip of silicon probes and
141 place them onto a clean aluminum stub (used for SEM-FIB imaging / etching) to prepare for
142 mounting.

144 1.5 Use a toothpick (or other fine tipped instrument like a thin electrical wire), to place a tiny
145 drop (~10 µL) of silver paint on the edge of the silicon substrate surrounding the probes. Secure
146 the strip down by spreading the silver paint around the sides of the silicon substrate surrounding
147 the probe. Allow the silver paint to dry completely before placing the aluminum stub into the
148 SEM-FIB.

150 NOTE: Be careful not to get silver paint on the shank of the electrode because that is the part
151 that will be etched. If the strip of probes is not securely anchored to the aluminum stub, the strip
152 may move during processing or have a different focal plane, thereby resulting in incorrect milling
153 by the FIB. Several strips of silicon probes can be mounted onto the same aluminum stub, making
154 sure there is ample space between the strips to allow for removal from the stub after etching.
155 This will allow more efficient etching of multiple probes using the automated feature described
156 below.

158 **2. Aligning the FIB to the silicon probes**

160 2.1 Click on **vent** button in the beam control tab to vent the chamber. Press **Shift+F3** to perform
161 home stage. Confirm the selection by selecting the **Home Stage** button in the popup window.

163 NOTE: Running the home stage operation is a preventative step to ensure the stage axis are read
164 correctly by the software and the microscope is in good condition.

166 2.2 After the Home Stage is complete, move the stage to coordinates X=70 mm, Y= 70 mm, Z = 0
167 mm, T=0°, R=0°. Once the chamber is vented, put on clean nitrile gloves and open the chamber
168 door.

170 NOTE: Depending on the previous user's application, it may be necessary to change the stage
171 adapter. The standard stage adapters (e.g., FEI style) can be removed by unscrewing the central
172 bolt counterclockwise and installed by screwing clockwise into the rotation plate of the stage.

174 2.3 Insert the aluminum stub holding the probes into the top of the stage adapter. Secure the
175 aluminum stub by tightening the set screw on the side of the stage adapter. Use the 1.5 mm hex
176 wrench for this task.

177

178 2.4 Adjust the height of the stage adapter by turning the adapter clockwise to lower it or
179 counterclockwise to raise it. Secure the stage adapter to the rotation plate by turning the locking
180 cone nut clockwise until the nut is secure against the stage rotation plate. Hold the stage adapter
181 with the other hand to prevent the rotation of the adapter and samples while tightening the
182 locking cone nut.

183

184 NOTE: Use the provided height gauge to determine the appropriate height. The top of the
185 aluminum stub should be the same height as the maximum line shown on the height gauge. Over
186 tightening the cone nut can cause damage to the stage and adapter. Only use enough force to
187 secure the samples.

188

189 2.5 Acquire a navigation camera image. Carefully swing the navigation camera arm open until it
190 stops. The microscope stage will automatically move to a position beneath the camera. Watch
191 the live image shown in Quadrant 3 of the microscope user interface (UI).

192

193 2.5.1 Once the brightness level auto adjusts to an appropriate level, acquire the image by pushing
194 the button down on the camera bracket. Be sure to wait for the entire image acquisition to finish,
195 which is indicated by a pause symbol appearing in Quadrant 3 and the illumination of the camera
196 turning off. This takes approximately 10 s. Swing the camera arm back to the closed position.
197 The stage will return to the original position.

198

199 2.6 Carefully close the microscope chamber door. Watch the CCD camera image in Quadrant 4
200 while closing the door. Ensure that the samples and stage are a safe distance away from any
201 critical component in the microscope chamber.

202

203 2.7 Select the down arrow next to the Pump button in the beam control tab. Select **Pump with**
204 **Sample Cleaning** button in the UI software to start the chamber vacuum pump and built in
205 plasma cleaner. Ensure the door is sealed by gently pushing on the face of the door while the
206 pump is running. Wait for approximately 8 min for the pumping time and plasma cleaning cycle
207 for the microscope chamber to be completed.

208

209 NOTE: A vacuum seal can be confirmed by gently pulling on the chamber door, which should
210 remain closed if the system is under vacuum.

211

212 2.8 Once the icon in the bottom right corner of the UI turns green, press the **Wake-Up** button in
213 the beam control tab which turns on the electron and ion beams. Select quadrant 1 and set the
214 beam signal to electron beam (if not set already), set quadrant 2 to ion beam (if not set already)

215

216 2.8.1 Set SEM voltage to 5 kV, set SEM beam current to 0.20 nA, set SEM detector to ETD, set
217 detector mode to Secondary Electron. Set FIB voltage to 30 kV, set FIB beam current to 24 pA,
218 set FIB detector to ICE detector, set detector mode to the secondary electron.

219

220 2.9 Double click on the **silicon probe** in the navigation camera image, quadrant 3 to move the
221 stage to the approximate location of the probe. Click on **quadrant 1** to select it as the active
222 quadrant and hit the pause button to start SEM scanning. Set the scan dwell time to 300 ns and
223 turn off **scan interlacing**, **line integration**, and **frame averaging**. Set scan rotation to 0 in the
224 beam control tab and right click on the beam shift 2d adjuster and select **zero**.
225
226 2.10 Adjust the magnification to the minimum value by turning the magnification knob
227 counterclockwise on the MUI panel. Adjust the image brightness and contrast using the knobs on
228 MUI panel or **the Auto Contrast Brightness** toolbar icon.
229
230 2.11 Move the stage by either double-left-clicking the mouse on a feature to center it, or by
231 pressing down the mouse wheel and activating the joystick mouse mode. Move the desired
232 silicon probe to be patterned into the center of the SEM image.
233
234 2.12 Locate an edge or other features such as a dust particle or scratch. Increase magnification
235 to 2000x by turning the magnification knob clockwise. Adjust the focus of the SEM by turning the
236 coarse and fine focus knobs on the MUI until the image is in focus. Once the image is in focus,
237 select the **Link sample Z to working distance** button in the toolbar.
238
239 2.13 Confirm that operation was completed by looking at the Z-axis coordinate in the navigation
240 tab. The value should be approximately 11 mm. Type in 4.0 mm in the Z axis position and push
241 the **Go To** button with the mouse or hit the enter key on the keyboard and the stage will move
242 to 4 mm working distance.
243
244 2.14 Move the stage in X and Y to locate the shoulder of the silicon probe. Position it as close to
245 the center of the SEM as possible. Change the stage tilt to 52˚ by typing in "52" in the T coordinate
246 and hitting enter. Observe whether the shoulder of the probe appears to move up or down in
247 the image. Use the Stage Z slider to bring the shoulder of the probe back to the center of the SEM
248 image. Only adjust the Z position, do not move X, Y, T, or R axis.
249
250 2.15 Run the built in "**xT Align Feature**" command located in the stage drop down menu. Use the
251 mouse to click on two points parallel to the edge of the probe. Make sure the horizontal radio
252 button is selected in the popup window and click finish. The stage will rotate to align the probe
253 with the X axis of the stage. Adjust the stage in X,Y using the mouse to put the lower shoulder of
254 the probe in the center of the SEM image again.
255
256 NOTE: The first point should be towards the probe's grip and the second point should be towards
257 the probe's point.
258
259 2.16 Select the FIB in quadrant 2 and make sure the beam current is still 24 pA. Set the
260 magnification to 5000x and the dwell time to 100 ns. Type **Ctrl-F** on the keyboard to set the FIB
261 focus to 13.0 mm. In the beam control tab, right click in the **stigmator 2d adjuster** and select **zero**
262 and, also, right click in the **Beam Shift 2d adjuster** and select **zero**. Set the scan rotation to 0° and
263 push the auto contrast brightness button in the toolbar.

264

265 2.17 Look for an image of the probe shoulder in quadrant 2. Use the **snapshot tool** to acquire an
266 image with the FIB. Confirm the probe shoulder is in the center of the FIB image, if not, double
267 click on the probe shoulder to move it to center. Move the stage to the left by pushing the left
268 arrow key on the keyboard approximately 10-15 times. Take another snapshot and observe
269 whether the probe side is still in the center of the FIB.
270

271 NOTE: IF not, the stage rotation must be adjusted slightly. If the probe is above the image center,
272 the stage must be rotated in the negative direction. If the probe is below center, the stage must
273 be rotated clockwise. Enter a relative compucentric rotation of 0.01 to 0.2 degrees depending on
274 which way is necessary to align the probe.
275

276 2.18 Repeat steps 2.16 to 2.17 as many times as necessary until the edge of the probe shoulder
277 is perfectly aligned with the X axis of the stage, (the edge stays in the center of the FIB while
278 moving left).
279

280 2.19 Using the FIB, move the stage back to the lower shoulder of the probe. Save the stage
281 position in the position list by clicking the **Add** button. Change the FIB beam current to 2.5 nA
282 and make sure the magnification of the FIB is still 5000x. Run the auto brightness contrast
283 function and set the FIB dwell time to 100 ns.
284

285 2.20 Hit the pause button to start scanning. Adjust the FIB focus and astigmatism, as quickly and
286 precisely as possible, using the Coarse and Fine focus knobs, and the X and Y stigmator knobs on
287 the MUI panel. Hit the pause button to stop the FIB scanning.
288

289 **3. Writing an automated process for etching.**
290

291 3.1 Start the software by locating it in the Windows start menu (i.e., Start\Programs\FEI
292 Company\Applications\Nanobuilder). Position the software window on the side monitor so the
293 UI is not covered up. Open the file for patterning the silicon probes by clicking **file** and then **open**.
294 Direct the windows browser to the location of the software script (**Supplementary File 1**-the file
295 name is "Case Western 2000 micron Final 11H47M runtime.jbj").
296

297 3.2 Within the software, select the microscope dropdown menu and select **Set stage origin**.
298 Within the software, select the microscope dropdown menu and then select **Calibrate Detectors**.
299

300 3.3 On the microscope UI, click in **Quad 1** once with the mouse to select Quad 1. Ignore the other
301 instructions shown in the popup window, they are not necessary for this project. Click **OK** to start
302 the calibration. The process will take about 5 min. Make sure the ETD and ICE detectors calibrate.
303 It is ok if any other detectors have calibration failures.
304

305 3.4 Within the software, select the microscope dropdown menu and choose **Execute** to start the
306 patterning sequence. When the pattern is complete, close the software.
307

308   NOTE: The software will take over quad 3 and 4 for the patterning and alignment functions. The
309   script will take approximately 12 h to run. While the script is running, do not change any
310   parameter on the microscope.
311
312   3.5 Hit "**Vent**" in the microscope UI beam control tab to shut down the microscope beams and
313   start the vent cycle. While the chamber is venting, move the stage to coordinates X=70 mm, Y=
314   70 mm, Z = 0 mm, T=0°, R=0°. Once the chamber is vented, put on clean nitrile gloves and pull
315   open the chamber door.
316
317   3.6 Loosen the set screw on the stub adapter using the 1.5 mm hex wrench. Remove the
318   aluminum stub containing the patterned probe from the chamber. Carefully close the microscope
319   chamber door. Watch the CCD camera image in Quadrant 4 while closing the door. Ensure that
320   the stage adapter is a safe distance away from any critical component in the microscope
321   chamber.
322
323   3.7 Select the **down arrow** next to the **Pump** button in the beam control tab. Select **Pump** button
324   to start the chamber vacuum pump. Ensure the door is sealed by gently pushing on the face of
325   the door while the pump is running.
326
327   NOTE: A vacuum seal can be confirmed by gently pulling on the chamber door, which should
328   remain closed if the system is under vacuum. The pumping time will be approximately 5 min.
329   Only one side of the probe can be etched during a single run.
330
331   3.8 If the front and back side of the probe requires etching, then carefully remove the etched
332   strip of silicon probes after checking the final etch and imaging the front side (if images are
333   needed). Dissolve the silver paint with acetone, by cautiously dabbing/brushing the acetone on
334   the silver paint. Carefully turn the strip around to the backside, re-mount, align and etch following
335   the steps described above.
336
337   **4. Checking the final etch and imaging**
338
339   4.1 Once the milling is complete verify the uniformity of the different sections using SEM imaging
340   at a higher magnification.
341
342   NOTE: Imaging at the tilted angle allows a better assessment of the variation in the milling depth.
343   Special attention should be given to the transition regions between the milling locations.
344
345   4.2 Image the samples again after milling with an optical microscope.
346
347   NOTE: The periodic milled lines result in a refraction effect giving rise to different colors as a
348   function of the imaging angle. If the color is not continuous along with the probe that is a clear
349   indication of the disruption in the milled lines.
350
351   **5. Mounting a functional silicon probe for FIB etching**

352
353 5.1 Gently remove the functional silicon electrode from its packaging. Use forceps to carefully lift
354 the plastic protective tab covering the head stage. Start lifting one corner of the tab up from the
355 sticky glue holding it in place and keep lifting until the entire electrode is removed.
356
357 5.2 Carefully clamp the electrode with hemostats to prepare for mounting into the stereotaxic
358 frame. While holding the covered tab with the forceps, gently place curved hemostats around
359 the green shaft above the silicon shank, with the curved part of the hemostats facing upwards
360 towards the tab. Lock the hemostats in place to ensure the electrode will not drop out of the
361 hemostats.
362
363 5.3 Gently remove the plastic protective tab covering the head stage. While holding the electrode
364 with the hemostats, carefully clip the electrode into the stereotaxic frame for cleaning.
365
366 5.4 Fill 3 Petri dishes with 95% ethanol (~10 mL per petri dish). Place the Petri dish under the
367 electrode that is mounted into the stereotaxic frame for cleaning. Slowly lower the electrode by
368 turning the micromanipulator downwards (100 µm/s) so that the shank is submerged into the
369 95% ethanol.
370
371 NOTE: Be careful not to turn the micromanipulator too fast or too deep, this can cause the
372 electrode to break (i.e., the electrode should not touch the Petri dish).
373
374 5.5 Leave the electrode shank in the 95% ethanol for 5 min, and then slowly raise the electrode
375 out of the 95% ethanol by turning the micromanipulator upwards (100 µm/s). Repeat this step
376 two more times, for a total of three washes. Allow the electrode to air dry for five minutes.
377
378 5.6 Use the same technique for mounting the electrode into the stereotaxic frame, to remove
379 the electrode from the stereotaxic frame. Carefully place the hemostats around the shaft of the
380 electrode. Once the hemostats are clasped tight, release the electrode from the stereotaxic
381 frame, return the plastic protective tab covering the head stage, and put the cleaned electrode
382 back into its packaging.
383
384 **6. Etching functional silicon probe using FIB**
385
386 6.1 Mount the cleaned functional silicon electrode onto an aluminum stand. Carefully pick up the
387 cleaned functional silicon electrode using forceps and remove the protective tab from the
388 headstage. Place the electrode shank on the aluminum stub so it does not hang over any edge,
389 then using a small piece of Cu or carbon conductive tape, pin the headstage securely to the
390 aluminum stub.
391
392 NOTE: Alternatively, a low-profile clip holder can be used to hold the electrode down. Be careful
393 not to touch the electrode shank.
394

395 6.2 Following the steps described above (Section 2), position the electrode at the eucentric height
396 and make sure the electrode is at the coincidence point of the SEM and FIB beams. Align the
397 shank with the "X"direction of the stage.
398
399 6.3 Set the FIB to the optimal current for milling the required the nano-architecture and make
400 sure the focus and stigmation are properly corrected. Prepare an array of lines with desired
401 spacing and length to cover the field of view of the shank (500 μm sections). Adjust the line
402 lengths as etching gets down the shank to the thinner sections.
403
404 NOTE: When etching the functional electrode, it is not possible to add fiducial marks to automate
405 the process. Therefore, moving between the sub-sections (~ 500 μm) is done manually.
406
407 6.4 After the milling of the first section is complete, make sure to check the milling quality before
408 moving on to the next section. Repeat step 6.3 to etch the next section of the shank. Align the
409 milled lines from the previous section to the patterns used for the next section to prevent large
410 gaps between runs.
411
412 **REPRESENTATIVE RESULTS:**
413
414 **FIB Etched Nano-architecture on the Surfaces of Single Shank Intracortical Probes**
415 Utilizing the methods described here, intracortical probes were etched with specific nano-
416 architectures following established protocols[39]. Dimensions and shape of the nano-architecture
417 design described in these methods were implemented from previous in vitro results depicting a
418 decrease in glial cell reactivity when cultured with the nano-architecture design described
419 here[37,38]. The methods described here utilized a focused gallium ion beam (FIB) to etch nanoscale
420 parallel grooves into the surface of non-functional single shank silicon microelectrode probes, as
421 previously described[39]. The nanoscale parallel grooves were etched along the shank of the
422 backside of the probe using an automated script written in the software. The final dimensions of
423 the etched nano-architecture were 200 nm wide parallel lines, spaced 300 nm apart, and had a
424 depth of 200 nm (**Figure 1**). The use of FIB to etch nano-architectures into a device surface allows
425 for etching of precise designs into manufactured devices.
426
427 **Etched Nano-architecture into Intracortical Probes Effect on Neuroinflammation**
428 In this previously reported data, the intracortical probes with etched nano-architectures were
429 implanted into the cortex of rats for either two or four weeks (n=4 per time point) and compared
430 to control animals implanted with smooth probes containing no nano-architecture etchings (n=4
431 per time point)[39]. One of the mechanisms of failure impeding the clinical deployment of
432 intracortical microelectrodes is the neuroinflammatory response induced from disrupting the
433 brain parenchyma and blood brain barrier[9-12,15]. A full description of the neuroinflammatory
434 response observed after intracortical microelectrode implantation can be found in the following
435 reviews[13,14,22]. The ability of intracortical microelectrodes to record action potentials from
436 neurons is dependent on the distance of the healthy neuronal bodies from the intracortical
437 microelectrode recording site[40]. Therefore, the previously reported study evaluated the
438 neuroinflammation around the intracortical probe implantation site by quantifying histological

439   markers for neuronal density, glial cell activation and gene expression of proinflammatory
440   markers[39]. Highlights from that study are presented below to represent the effects etching nano-
441   architectures into the probe surface had on neuroinflammation.
442
443   **Effects of Etched Nano-architecture on Neuron Density**
444   To determine how etching nano-architectures into the probe's surface effects the neuronal
445   density immediately around the implant, the neuronal nuclei were stained and quantified
446   utilizing previously describing immunohistochemistry methods[39,41]. There were no significant
447   differences of neuron densities around the nano-architecture and control probes at 2 weeks post
448   implantation (**Figure 2A**). However, there were significantly more neurons around the nano-
449   architecture probes at 100–150 µm distance from the implant site compared to the smooth
450   control implants (p < 0.05 vs controls) (**Figure 2B**) at 4 weeks post implantation. It was also found
451   that there was an increased trend of neuronal density surrounding the nano-architecture probes
452   over time, contrasting the decreased trend of neuronal density around the control implants
453   (**Figure 2**). There is a direct relationship depicting a mitigated neuroinflammatory response
454   coupled with a higher density of viable neurons surrounding the microelectrode, results in an
455   increased ability for the microelectrode to provide quality recordings[15,40,42]. Therefore, when
456   interpreting neuronal density data, a higher density of neurons around the implant site may
457   indicate a lessened neuroinflammatory response and potentially improved recording quality and
458   stability from intracortical microelectrodes.
459
460   **Effects of Etched Nano-architecture on Neuroinflammatory Molecular Markers**
461   Histology is enough for identifying the cells around an implant site; however, it lacks the
462   sensitivity and specificity for characterizing the phenotype of the surrounding cells. Hence,
463   methods utilizing quantitative gene expression analysis were employed to quantify the relative
464   gene expression of neuroinflammatory markers, in order to understand the effect nano-
465   architecture has on the phenotype of the cells[39]. Several neuroinflammatory markers were
466   investigated in the previously reported study. Here only two will be highlighted that are specific
467   to microglia cells, in order to discuss how their phenotype may have been altered. The cluster of
468   differentiation 14 (CD14) is a pattern recognition receptor on the membrane of microglia that
469   recognizes bacteria and signals the inflammatory pathway after injury/implantation[43-45]. Nitric
470   oxide synthase (NOS2), is an oxidative stress marker expressed in microglia/macrophages that is
471   associated with an increased production of proinflammatory markers[46,47].
472
473   In the previously reported data, there were no significant differences of CD14 relative gene
474   expression between nano-architecture and control implants at either two- or four-weeks post-
475   implantation. Notably, there was a significant decrease (p < 0.05) of CD14 relative gene
476   expression from two to four weeks around the nano-architecture implants' site, indicating a
477   possible decrease in inflammation (denoted by * in **Figure 3A**). Similarly, were no significant
478   differences of NOS2 relative gene expression between nano-architecture and control implants at
479   two weeks. However, there was significantly less (p < 0.05) NOS2 relative gene expression around
480   the nano-architecture implant compared to the control implant at four weeks post-implantation
481   (denoted by # in **Figure 3B**). Moreover, there was a significant increase from 2 to 4 weeks of NOS2
482   relative gene expression around the control implants (denoted by * in **Figure 3B**), and no

483 differences observed around the nano-architecture implants over time, further indicating a
484 potential decrease of inflammation around the nano-architecture implants. When interpreting
485 this data, it is important to understand the function of the gene being quantified. For example,
486 decreases of pro-inflammatory genes indicate a probable decrease in the inflammatory response
487 around the electrode site, whereas an increase in these types of genes suggests a likely increase
488 in inflammation.
489
490 **FIB Etched Nano-architecture on the Surfaces of Functional Single Shank Microelectrodes**
491 The previously reported study had promising results demonstrating a slight increase of neuron
492 density and the potential decrease in microglia inflammatory phenotype around the nano-
493 architecture probe implant site. To investigate the translation of these results to electrode
494 functionality, a functional single shank silicon microelectrode was etched with the same nano-
495 architecture design as the non-functional single shank silicon microelectrode probes, utilizing a
496 similar FIB etching protocol. The only difference in the methodology for etching the specified
497 nano-architecture was that the protocol for the functional electrodes could not be automated,
498 as there was no extra substrate material to create fiducial markings. Thus, the functional
499 electrode was manually etched using FIB by re-aligning the beam every 500 μm, as described in
500 the protocol above. The final etchings were 200 nm wide parallel lines, spaced 300 nm apart, and
501 had a depth of 200 nm (**Figure 4**).
502
503 **Effects of Etched Nano-architecture into Intracortical Microelectrodes on Electrophysiology**
504 Successful intracortical microelectrode recordings are reliant on the proximity of the neurons
505 around the implant sites, the integrity of the device and the reliable transmission of single unit
506 activity from the brain[8,40,48,49]. Electrophysiological recordings were quantified utilizing recorded
507 metrics collected twice per week over eight weeks. The metrics utilized in this study were, the
508 percentage of channels recording single units, maximum amplitudes of recorded units, and
509 signal-to-noise ratio (SNR). The Institutional Animal Care and Use Committees (IACUC) at the
510 Louis Stokes Cleveland Veterans Affairs Medical Center approved all animal procedures. Sprague
511 Dawley rats (8-10 weeks old and weighing ~225 g) were implanted with single shank silicon
512 microelectrode, with the above-mentioned nano-architecture (n=1) or the smooth controls
513 (n=6). No statistical analysis was performed on this data, as there was one nano-architecture
514 microelectrode implanted for a proof-of-concept pilot study. Nonetheless, collective
515 electrophysiological results showing an increased percentage of channels recording single units
516 (**Figure 5A**), maximum amplitudes (**Figure 5B**) of recorded units, and SNR (**Figure 5C**) from the
517 nano-architecture microelectrodes compared to the smooth control microelectrodes, are
518 promising. These results indicate that the etching of nano-architecture into the surface of
519 microelectrodes may potentially result in improved quality and increased longevity of
520 electrophysiological recordings. Further evaluation with increased sample size is necessary to
521 verify these preliminary findings.
522
523 **FIGURE AND TABLE LEGENDS:**
524
525 **Figure 1: FIB Etched Nano-architecture on the Surfaces of Single Shank Intracortical Probes.**
526 SEM images of the non-functional single shank silicon probes with FIB etched nano-architectures

527 along the backside of the shank. (**A**) Composite images of the entire probe post etching shown at
528 120x magnification (scale bar is 400 μm). The fiducial marks, (square box with a + symbol going
529 through it), are etched along the silicon substrate surrounding the probe. Magnified SEM images
530 of the probe tip are shown in (**B**) at 1056× magnification (scale bar is 40 μm), (**C**) at 3500x
531 magnification (scale bar is 10 μm), and (**D**) at 10,000x magnification (scale bar is 4 μm). This figure
532 has been modified from[39].

533

534 **Figure 2: Effects of Etched Nano-architecture on Neuron Density.** Neuronal survival is presented
535 as a percentage of the background region from the same animals in distances of 50 μm bins away
536 from the implant site. (**A**) No significant differences of neuronal survival were observed between
537 the smooth surfaces (control) and nanopatterned implants at 2 weeks post-implantation. (**B**)
538 There was a significantly higher neuronal survival around the nanopatterned implants at the 100-
539 150 μm distance compared to smooth surfaces (p< 0.05) at 4 weeks post-implantation.
540 Representative images of neurons (stained green), with the yellow outline depicting the
541 implantation site, and the "P" denoting the etched side of the microelectrode (scale bar is 100
542 μm). This figure has been modified from[39].

543

544 **Figure 3: Effects of Etched Nano-architecture on Neuroinflammatory Molecular Markers.** Tissue
545 was collected around 500 μm radius of the implantation site for both the nanopatterned and
546 control implants. Relative gene expression of inflammatory markers was quantitatively compared
547 between both implant types (the differences are denoted by # on the graph; p<0.05) as well as
548 over time (the differences are denoted by * on the graph; p<0.05). (**A**) Relative gene expression
549 of CD14 significantly decreased around nanopatterned implants from two to four weeks (*). (**B**)
550 There was a significantly lesser relative gene expression of NOS2 around nanopattern implant
551 compared to control at four weeks (#) and there was a significant increase of NOS2 from two to
552 four weeks around smooth control implants (*). This figure has been modified from[39].

553

554 **Figure 4: FIB Etched Nano-architecture on the Surfaces of Functional Single Shank**
555 **Microelectrodes.** The inset on the top right corner displays the microelectrode utilized in this
556 study next to a dime to portray the size of the electrode shank (thin black line). SEM images of
557 the microelectrodes shank with FIB etched nano-architectures along the backside of the shank.
558 The entire shank is shown at the top at 600x magnification (scale bar is 50 μm), while the inset
559 depicts the nanopatterned surface at 25,000x magnification (scale bar is 1 μm).

560

561 **Figure 5: Effects of Etched Nano-architecture into Intracortical Microelectrodes on**
562 **Electrophysiology.** Evaluation of electrophysiological metrics discovered a promising preliminary
563 increased trend of (**A**) percentage of channels recording single units, (**B**) maximum amplitudes of
564 recorded units, and (**C**) signal-to-noise ratio from the microelectrode etched with nano-
565 architectures compared to the smooth control electrodes.

566

567 **Figure 6: Electrophysiology Recording from Implanted Functional Single Shank Microelectrodes**
568 **with FIB Etched Nano-architectures**. One of the challenges of using FIB to etch nano-
569 architectures on manufactured microelectrode devices is the risk of short-circuiting recording
570 contacts. The x-axis depicts the recording time in seconds, and the y-axis shows the electrode

571   channels recording neuronal action potentials. Each numbered line on the y-axis represents a
572   different electrode channel, with channel number 1 being the shallowest and 16 being the
573   deepest. The red boxes outline the short-circuited channels, whereas the blue boxes outline
574   channels with visible neuronal activity.
575

576   **DISCUSSION:**
577   The fabrication protocol outlined here utilizes focused ion beam lithography to effectively and
578   reproducibly etch nano-architectures into the surface of non-functional and functional single
579   shank silicon microelectrodes. Focused ion beam (FIB) lithography allows for the selective
580   ablation of the substrate surface by using a finely-focused ion beam[50,51]. FIB is a direct–write
581   technique that can produce various features with nanoscale resolution and high aspect
582   ratio[50,52,53]. In order to create the various sized features, the magnitude of the ion beam current
583   can be optimized to change the ion beam spot size within a range of 3 nm to 2 µm[50,51]. Some
584   general advantages of using FIB to etch features onto surfaces are: 1) it can be used on a wide
585   variety of materials, including silicon, metals, and polymers[53-56], 2) FIB can be performed on non-
586   planar surfaces, and 3) FIB can be used for post-processing on individual devices[57].
587

588   Here, FIB was used in combination with an SEM microscope and software used to write a
589   specialized automated script for etching specific features into non-functional single shank
590   probes. The script included parameters required (2.5 nA ion beam current and 30 kV voltage) to
591   etch the exact spacing desired (200 nm wide parallel grooves, spaced 300 nm apart and 20 nm
592   deep). The dimensions of the electrode exceeded the field of view for the FIB, so the patterning
593   was performed in multiple stage positions. In order to automate the process, fiducial marks were
594   etched into the side of the silicon sheet holding the probes in place, to allow the software to
595   precisely locate the patterned lines on the probe shank. The fiducials were necessary because
596   the stage motion created a large (~5 µm) uncertainty in the location of the pattern area with
597   respect to the ion beam field of view. Placement of the fiducials on the silicon sheet allowed for
598   the FIB to locate the pattern areas without directly scanning the beam on the probe shank, which
599   could potentially contaminate or damage the probe shank. The entire automated etching process
600   for one shank took approximately 12 h to complete and required no operator intervention after
601   the patterning was started. Collectively, the benefits of using FIB to etch features into the silicon
602   probe shank were the ability to make nanometer sized features, automate the etching process,
603   and the capacity to etch on a fabricated probe. Although FIB has copious benefits, one of the
604   drawbacks of using this fabrication method is the slow throughput rate that ultimately limits the
605   potential for mass production of devices with nano-architectures into their surface[58].
606   Alternatively, other fabrication methods utilized to create feature sizes and geometries of
607   interest, perhaps at faster rates and at mass productions, include electron beam lithography and
608   nanoimprint lithography[59-65]. However, these methods do not allow for etching of nano-
609   architecture features into manufactured devices. Traditionally these methods are utilized during
610   the fabrication process on a sheet of silicon or polymer, which can then be used in downstream
611   processing steps to fabricate the final deceive.
612

613   The functional electrodes were unable to undergo an automated process due to not having any
614   surrounding material around the electrode shank in which to include fiducial marks into the run.

615   Therefore, the functional electrodes were manually aligned and etched at 500 μm sections along
616   the shank, using the same ion current and voltage as the automated run to ensure the same
617   feature sizes. The beam had to be manually realigned after completing each 500 μm interval and
618   set up to etch the next section. The process of manual realignment of the patterns every 500 μm
619   can potentially lead to damaged nanostructures or structures that do not match the intended
620   geometry. This is due to longer exposure times the ion beam needs for manual alignment[66]. This
621   was one of the difficulties encountered with the manual etching. Due to this complication, two
622   recording contacts were short-circuited and were unable to record neuronal action potentials
623   (**Figure 6**). **Figure 6** demonstrates an electrophysiological live recording segment from the animal
624   implanted with the nano-architecture electrode. The blue boxes outline the channels recording
625   strong action potentials, in comparison to the red boxes denoting the two dead channels. Hence,
626   one of the challenges of using manual FIB etching on post-manufactured electrodes is that there
627   is a chance that the beam can short-circuit contacts and prevent them from recording. This
628   challenge is enhanced when attempting to etch the front side of single shank silicon electrodes,
629   in which the recording contacts and traces are along the entire shank of the electrode. Although
630   it is feasible to etch the silicon around the recording contacts and traces, extra caution is advised
631   to avoid damage and decreased performance of recording capabilities of the electrode.
632
633   As previously mentioned, FIB can be utilized on various materials to etch numerous feature
634   geometries into the surface. However, it is important to note that the parameters to etch
635   geometries, such as lines into the various materials, are complicated to predict. Particularly for
636   line patterns, the line width and depth are strongly dependent on many parameters such as the
637   accelerating voltage, beam current, dwell time, pixel spacing, lifetime of the aperture and
638   material type. Another parameter that results from the optimization is total time to mill each
639   line. Narrower and deeper lines could be achieved using smaller beam currents; however, the
640   pattern time for an entire probe shank would extend to multiple days, which is not practical.
641   Thus, although it is feasible to optimize the protocol presented here, it would be exceedingly
642   difficult to describe the parameters for unknown materials. In troubleshooting the parameters
643   for the silicon probes described in this protocol, numerous test cuts in silicon were made to
644   evaluate how the changing conditions affected the line width and depths. As soon as the
645   evaluated conditions were able to etch the specific feature size and geometry of interest (200
646   nm wide lines that were 200 nm deep), those parameters were used to write the software script.
647   The script was used to control the spacing of each line, from center to center, which in this
648   protocol is 300 nm. Future studies utilizing silicon substrates/devices requiring feature sizes in
649   the hundreds of nanometers, can use the parameters described in this protocol as a starting point
650   for troubleshooting the conditions needed to create the desired feature sizes. Further
651   optimization and troubleshooting of the etching conditions will be required for metal and
652   polymer substrates/devices. Overall, utilizing FIB for etching nano-architectures into material
653   surfaces allows for ample control and flexibility in feature geometries, use of numerous
654   compatible materials, and several surface types, including manufactured devices. Representative
655   results presented herein demonstrated the potential benefits observed in our studies of utilizing
656   FIB to etch nano-architectures into the surface of intracortical microelectrodes: 1) increased
657   neuronal density and 2) reduction of neuroinflammatory markers around implanted devices with
658   nano-architectures, as well as 3) preliminary findings depicting improved quality of

659 electrophysiological recordings over time. Likewise, the employment and optimization of the
660 described protocol etching nano-architecture features into the surface of a material can be
661 utilized to improve the functionality of numerous medical devices.
662

670

671 **DISCLOSURES:**
672 The authors have nothing to disclose.
673

674

675 **REFERENCES:**
676 1   Salcman, M., Bak, M. J. A new chronic recording intracortical microelectrode. *Medical and*
677 *Biological Engineering.* **14** (1), 42-50, (1976).
678 2   Im, C., Seo, J.-M. A review of electrodes for the electrical brain signal recording.
679 *Biomedical Engineering Letters.* **6** (3), 104-112, (2016).
680 3   Donoghue, J. Bridging the Brain to the World: A Perspective on Neural Interface Systems.
681 *Neuron.* **60** (3), 511-521, (2008).
682 4   Gilja, V. et al. Clinical translation of a high-performance neural prosthesis. *Nature*
683 *medicine.* **21** (10), 1142-1145, (2015).
684 5   Wolpaw, J. R., McFarland, D. J. Control of a two-dimensional movement signal by a
685 noninvasive brain-computer interface in humans. *Proceedings of the National Academy of*
686 *Sciences.* **101** (51), 17849-17854, (2004).
687 6   Ajiboye, A. B. et al. Restoration of reaching and grasping in a person with tetraplegia
688 through brain-controlled muscle stimulation: a proof-of-concept demonstration. *Lancet.* **389**
689 (10081):1821-1830 (2017).
690 7   Polikov, V. S., Tresco, P. A., Reichert, W. M. Response of brain tissue to chronically
691 implanted neural electrodes. *Journal of Neuroscience Methods.* **148** (1), 1-18, (2005).
692 8   Barrese, J. C. et al. Failure mode analysis of silicon-based intracortical microelectrode
693 arrays in non-human primates. *Journal of Neural Engineering.* **10** (6), 066014, (2013).
694 9   McConnell, G. C. et al. Implanted neural electrodes cause chronic, local inflammation that
695 is correlated with local neurodegeneration. *Journal of Neural Engineering.* **6** (5), 056003, (2009).
696 10   Potter, K. A., Buck, A. C., Self, W. K., Capadona, J. R. Stab injury and device implantation
697 within the brain results in inversely multiphasic neuroinflammatory and neurodegenerative
698 responses. *Journal of Neural Engineering.* **9** (4), 046020, (2012).
699 11   Biran, R., Martin, D. C., Tresco, P. A. Neuronal cell loss accompanies the brain tissue
700 response to chronically implanted silicon microelectrode arrays. *Experimental Neurology.* **195** (1),
701 115-126, (2005).
702 12   Kozai, T. D., Jaquins-Gerstl, A. S., Vazquez, A. L., Michael, A. C., Cui, X. T. Brain tissue

responses to neural implants impact signal sensitivity and intervention strategies. *ACS Chemical Neurosciences.* **6** (1), 48-67, (2015).

13   Jorfi, M., Skousen, J. L., Weder, C., Capadona, J. R. Progress towards biocompatible intracortical microelectrodes for neural interfacing applications. *Journal of Neural Engineering.* **12** (1), 011001, (2015).

14   Michelson, N. J. et al. Multi-scale, multi-modal analysis uncovers complex relationship at the brain tissue-implant neural interface: new emphasis on the biological interface. *Journal of Neural Engineering.* **15** (3), 033001, (2018).

15   Saxena, T. et al. The impact of chronic blood-brain barrier breach on intracortical electrode function. *Biomaterials.* **34** (20), 4703-4713, (2013).

16   Potter, K. A. et al. The effect of resveratrol on neurodegeneration and blood brain barrier stability surrounding intracortical microelectrodes. *Biomaterials.* **34** 7001-7015, (2013).

17   Ravikumar, M. et al. The Roles of Blood-derived Macrophages and Resident Microglia in the Neuroinflammatory Response to Implanted Intracortical Microelectrodes. *Biomaterials.* **S0142-9612** (35), 8049-8064, (2014).

18   Hermann, J., Capadona, J. Understanding the Role of Innate Immunity in the Response to Intracortical Microelectrodes. *Critical Reviews in Biomedical Engineering.* **46** (4), 341-367 (2018)

19   Ereifej, E. S. et al. Implantation of Intracortical Microelectrodes Elicits Oxidative Stress. *Frontiers in Bioengineering and Biotechnology.* https://doi.org/10.3389/fbioe.2018.00009 (2018).

20   Block, M. L., Zecca, L., Hong, J. S. Microglia-mediated neurotoxicity: uncovering the molecular mechanisms. *Nature Reviews Neuroscience.* **8** (1), 57-69, (2007).

21   Nguyen, J. K. et al. Influence of resveratrol release on the tissue response to mechanically adaptive cortical implants. *Acta Biomaterialia.* **29** 81-93, (2016).

22   Salatino, J. W., Ludwig, K. A., Kozai, T. D., Purcell, E. K. Glial responses to implanted electrodes in the brain. *Nature Biomedical Engineering.* **1** (11), 862, (2017).

23   Block, M. L., Zecca, L., Hong, J.-S. Microglia-mediated neurotoxicity: uncovering the molecular mechanisms. *Nature Reviews Neuroscience.* **8** (1), 57-69, (2007).

24   Biran, R., Martin, D., Tresco, P. Neuronal cell loss accompanies the brain tissue response to chronically implanted silicon microelectrode arrays. *Experimental Neurology.* **195** (1), 115-126, (2005).

25   Liu, X. et al. Stability of the interface between neural tissue and chronically implanted intracortical microelectrodes. *IEEE Transactions on Rehabilitation Engineering.* **7** (3), 315-326, (1999).

26   Ereifej, E. S. et al. The Neuroinflammatory Response to Nanopatterning Parallel Grooves into the Surface Structure of Intracortical Microelectrodes. *Advanced Functional Materials.* 10.1002/adfm.201704420, (2017).

27   Nguyen, J. K. et al. Mechanically-compliant intracortical implants reduce the neuroinflammatory response. *Journal of Neural Engineering.* **11** (5), 056014, (2014).

28   Wei, X. et al. Nanofabricated Ultraflexible Electrode Arrays for High-Density Intracortical Recording. *Advanced Science.* 1700625, (2018).

29   Patel, P. R. et al. Chronic in vivo stability assessment of carbon fiber microelectrode arrays. *Journal of Neural Engineering.* **13** (6), 066002, (2016).

30   Chen, R., Canales, A., Anikeeva, P. Neural recording and modulation technologies. *Nature*

747 *Reviews Materials.* **2** (2), 16093, (2017).

31   Kim, Y. et al. Nano-Architectural Approaches for Improved Intracortical Interface Technologies. *Frontiers in Neuroscience.* **12**, (2018).

32   Millet, L. J., Bora, A., Sweedler, J. V. & Gillette, M. U. Direct cellular peptidomics of supraoptic magnocellular and hippocampal neurons in low-density co-cultures. *ACS Chemical Neurosciences.* **1** (1), 36-48, (2010).

33   Ding, H., Millet, L. J., Gillette, M. U., Popescu, G. Actin-driven cell dynamics probed by Fourier transform light scattering. *Biomedical Optical Express.* **1** (1), 260-267, (2010).

34   Kotov, N. A. et al. Nanomaterials for Neural Interfaces. *Advanced Materials.* **21** (40), 3970-4004, (2009).

35   Curtis, A. S. et al. Cells react to nanoscale order and symmetry in their surroundings. *IEEE Trans Nanobioscience.* **3** (1), 61-65, (2004).

36   Zervantonakis, I. K., Kothapalli, C. R., Chung, S., Sudo, R., Kamm, R. D. Microfluidic devices for studying heterotypic cell-cell interactions and tissue specimen cultures under controlled microenvironments. *Biomicrofluidics.* **5** (1), 13406, (2011).

37   Ereifej, E. S. et al. Nanopatterning effects on astrocyte reactivity. *Journal of Biomedical Materials Research Part A.* **101A** (6), 1743-1757, (2013).

38   Ereifej, E. S., Cheng, M. M.-C., Mao, G., VandeVord, P. J. Examining the inflammatory response to nanopatterned polydimethylsiloxane using organotypic brain slice methods. *Journal of Neuroscience Methods.* **217** (1-2), 17-25, (2013).

39   Ereifej, E. S. et al. The Neuroinflammatory Response to Nanopatterning Parallel Grooves into the Surface Structure of Intracortical Microelectrodes. *Advanced Functional Materials.* **28** (12), 1704420, (2018).

40   Buzsáki, G. Large-scale recording of neuronal ensembles. *Nature Neuroscience.* **7** (5), 446-451, (2004).

41   Mullen, R. J., Buck, C. R., Smith, A. M. NeuN, a neuronal specific nuclear protein in vertebrates. *Development.* **116** (1), 201-211, (1992).

42   Rennaker, R. L., Miller, J., Tang, H., Wilson, D. A. Minocycline increases quality and longevity of chronic neural recordings. *Journal of Neural Engineering.* **4** (2), L1-5, (2007).

43   Sladek, Z., Rysanek, D. Expression of macrophage CD14 receptor in the course of experimental inflammatory responses induced by lipopolysaccharide and muramyl dipeptide. *Veterinarni Medicina.* **53** (7), 347-357, (2008).

44   Janova, H. et al. CD14 is a key organizer of microglial responses to CNS infection and injury. *Glia.* (2015).

45   Ziegler-Heitbrock, H. W. L., Ulevitch, R. J. CD14: Cell surface receptor and differentiation marker. *Immunology Today.* **14** (3), 121-125, (1993).

46   Lowenstein, C. J., Padalko, E. iNOS (NOS2) at a glance. *Journal of Cell Science.* **117** (14), 2865-2867, (2004).

47   Aktan, F. iNOS-mediated nitric oxide production and its regulation. *Life Sciences.* **75** (6), 639-653, (2004).

48   Kozai, T. D. et al. Comprehensive chronic laminar single-unit, multi-unit, and local field potential recording performance with planar single shank electrode arrays. *Journal of Neurosciences Methods.* **242** 15-40, (2015).

49   Kozai, T. D. et al. Mechanical failure modes of chronically implanted planar silicon-based

791   neural probes for laminar recording. *Biomaterials.* **37** 25-39, (2015).

792   50   Raffa, V., Vittorio, O., Pensabene, V., Menciassi, A., Dario, P. FIB-nanostructured surfaces
793   and investigation of bio/nonbio interactions at the nanoscale. *IEEE Transactions on*
794   *Nanobioscience.* **7** (1), 1-10, (2008).

795   51   Lehrer, C., Frey, L., Petersen, S., Ryssel, H. Limitations of focused ion beam
796   nanomachining. *Journal of Vacuum Science & Technology B: Microelectronics and Nanometer*
797   *Structures Processing, Measurement, and Phenomena.* **19** (6), 2533-2538, (2001).

798   52   Watkins, R., Rockett, P., Thoms, S., Clampitt, R., Syms, R. Focused ion beam milling.
799   *Vacuum.* **36** (11-12), 961-967, (1986).

800   53   Veerman, J., Otter, A., Kuipers, L., Van Hulst, N. High definition aperture probes for near-
801   field optical microscopy fabricated by focused ion beam milling. *Applied Physics Letters.* **72** (24),
802   3115-3117, (1998).

803   54   Lanyon, Y. H., Arrigan, D. W. Recessed nanoband electrodes fabricated by focused ion
804   beam milling. *Sensors and Actuators B: Chemical.* **121** (1), 341-347, (2007).

805   55   Menard, L. D., Ramsey, J. M. Fabrication of sub-5 nm nanochannels in insulating
806   substrates using focused ion beam milling. *Nano Letters.* **11** (2), 512-517, (2010).

807   56   Ziberi, B., Cornejo, M., Frost, F., Rauschenbach, B. Highly ordered nanopatterns on Ge and
808   Si surfaces by ion beam sputtering. *Journal of Physics: Condensed Matter.* **21** (22), 224003, (2009).

809   57   Reyntjens, S., Puers, R. A review of focused ion beam applications in microsystem
810   technology. *Journal of Micromechanics and Microengineering.* **11** (4), 287, (2001).

811   58   Heyderman, L., David, C., Kläui, M., Vaz, C., Bland, J. Nanoscale ferromagnetic rings
812   fabricated by electron-beam lithography. *Journal of Applied Physics.* **93** (12), 10011-10013,
813   (2003).

814   59   Baquedano, E., Martinez, R. V., Llorens, J. M., Postigo, P. A. Fabrication of Silicon
815   Nanobelts and Nanopillars by Soft Lithography for Hydrophobic and Hydrophilic Photonic
816   Surfaces. *Nanomaterials.* **7** (5), 109, (2017).

817   60   Eom, H. et al. Nanotextured polymer substrate for flexible and mechanically robust metal
818   electrodes by nanoimprint lithography. *ACS Applied Materials & Interfaces.* **7** (45), 25171-25179,
819   (2015).

820   61   Li, K., Morton, K., Veres, T., Cui, B. 5.11 Nanoimprint Lithography and Its Application in
821   Tissue Engineering and Biosensing. *Comprehensive Biotechnology.* 125-139, (2011).
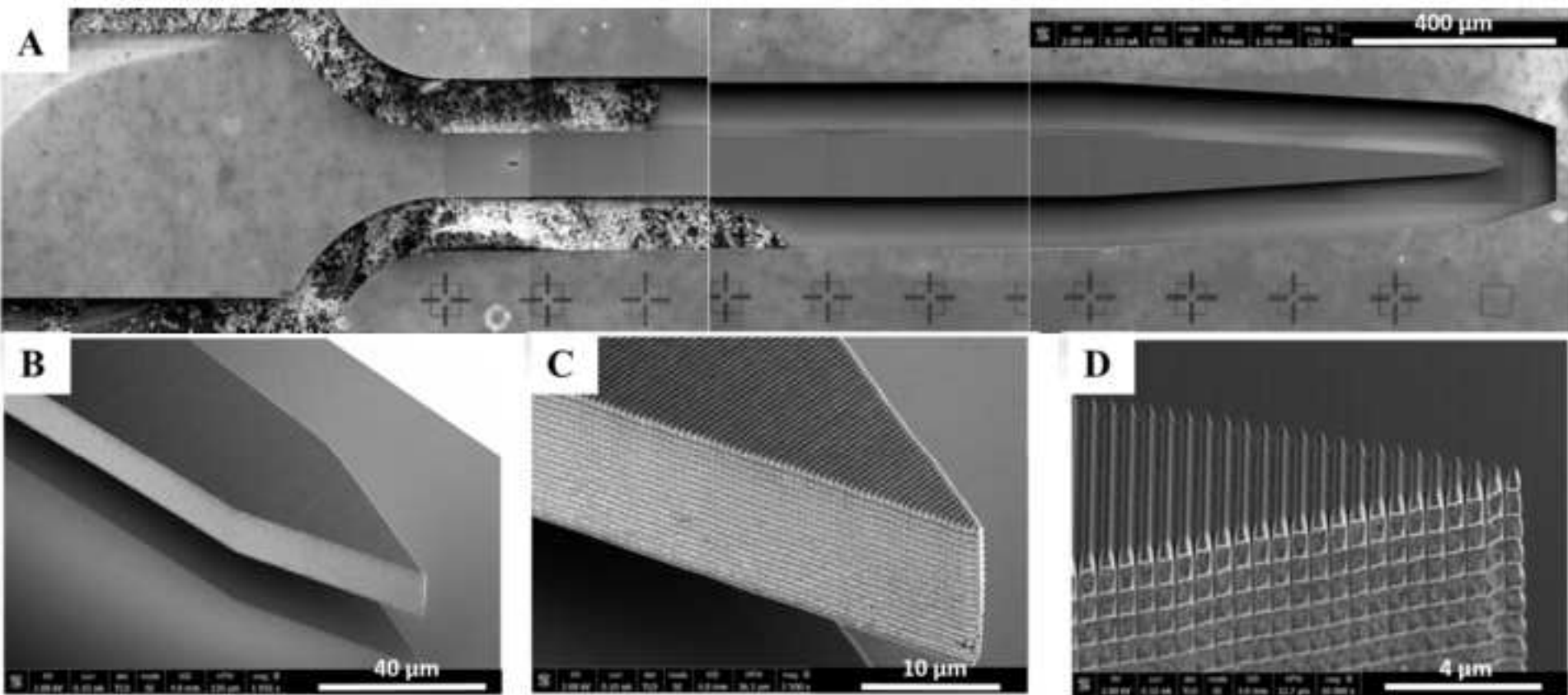
822   62   Dong, B., Zhong, D., Chi, L., Fuchs, H. Patterning of conducting polymers based on a
823   random copolymer strategy: Toward the facile fabrication of nanosensors exclusively based on
824   polymers. *Advanced Materials.* **17** (22), 2736-2741, (2005).
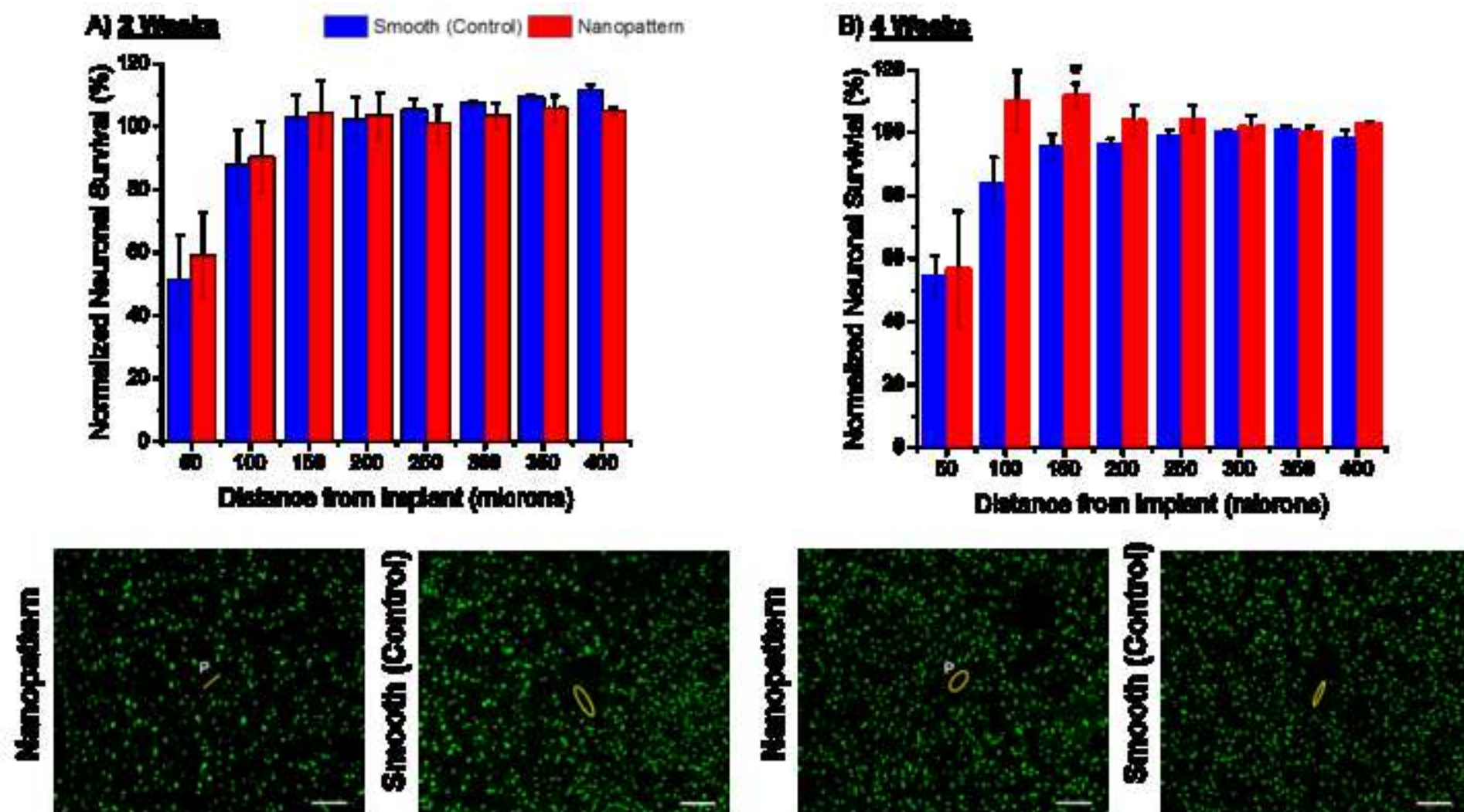
825   63   Dalby, M. J., Gadegaard, N., Wilkinson, C. D. The response of fibroblasts to hexagonal
826   nanotopography fabricated by electron beam lithography. *Journal of Biomedical Materials*
827   *Research Part A.* **84** (4), 973-979, (2008).

828   64   Tseng, A. A., Chen, K., Chen, C. D., Ma, K. J. Electron beam lithography in nanoscale
829   fabrication: recent development. *IEEE Transactions on Electronics Packaging Manufacturing.* **26**
830   (2), 141-149, (2003).

831   65   Yang, Y., Leong, K. W. Nanoscale surfacing for regenerative medicine. *Wiley*
832   *Interdisciplinary Reviews: Nanomedicine and Nanobiotechnology.* **2** (5), 478-495, (2010).

833   66   Vermeij, T., Plancher, E., Tasan, C. Preventing damage and redeposition during focused
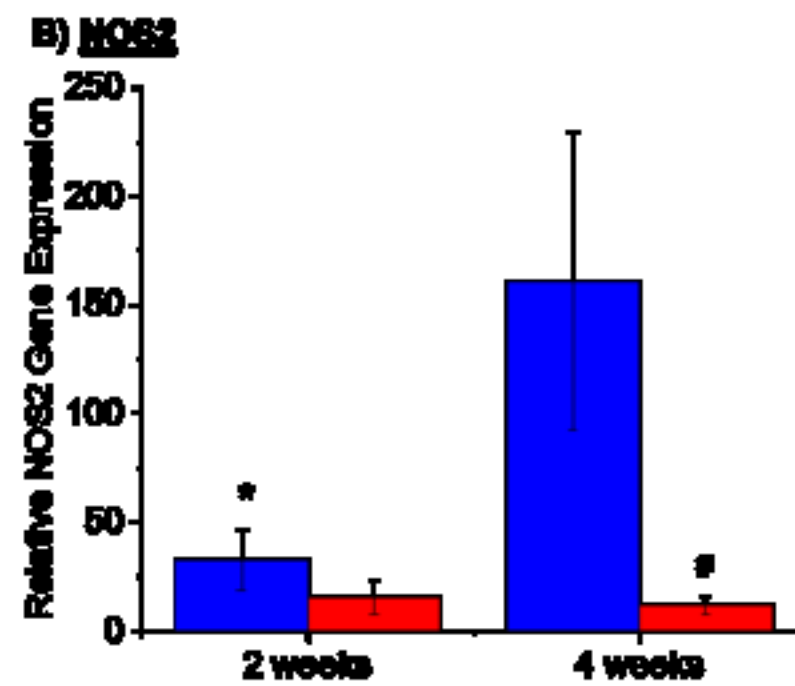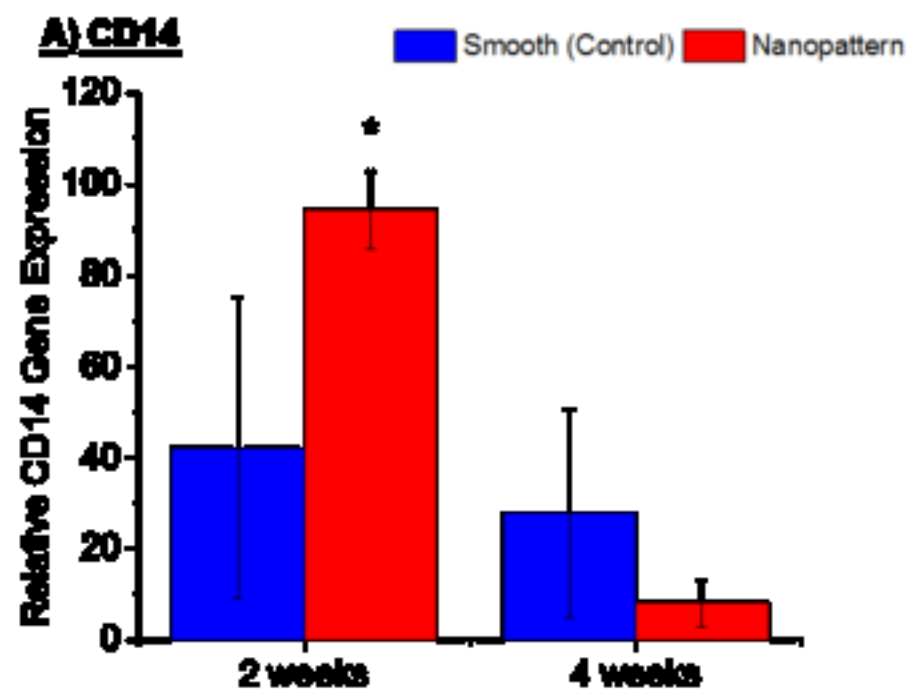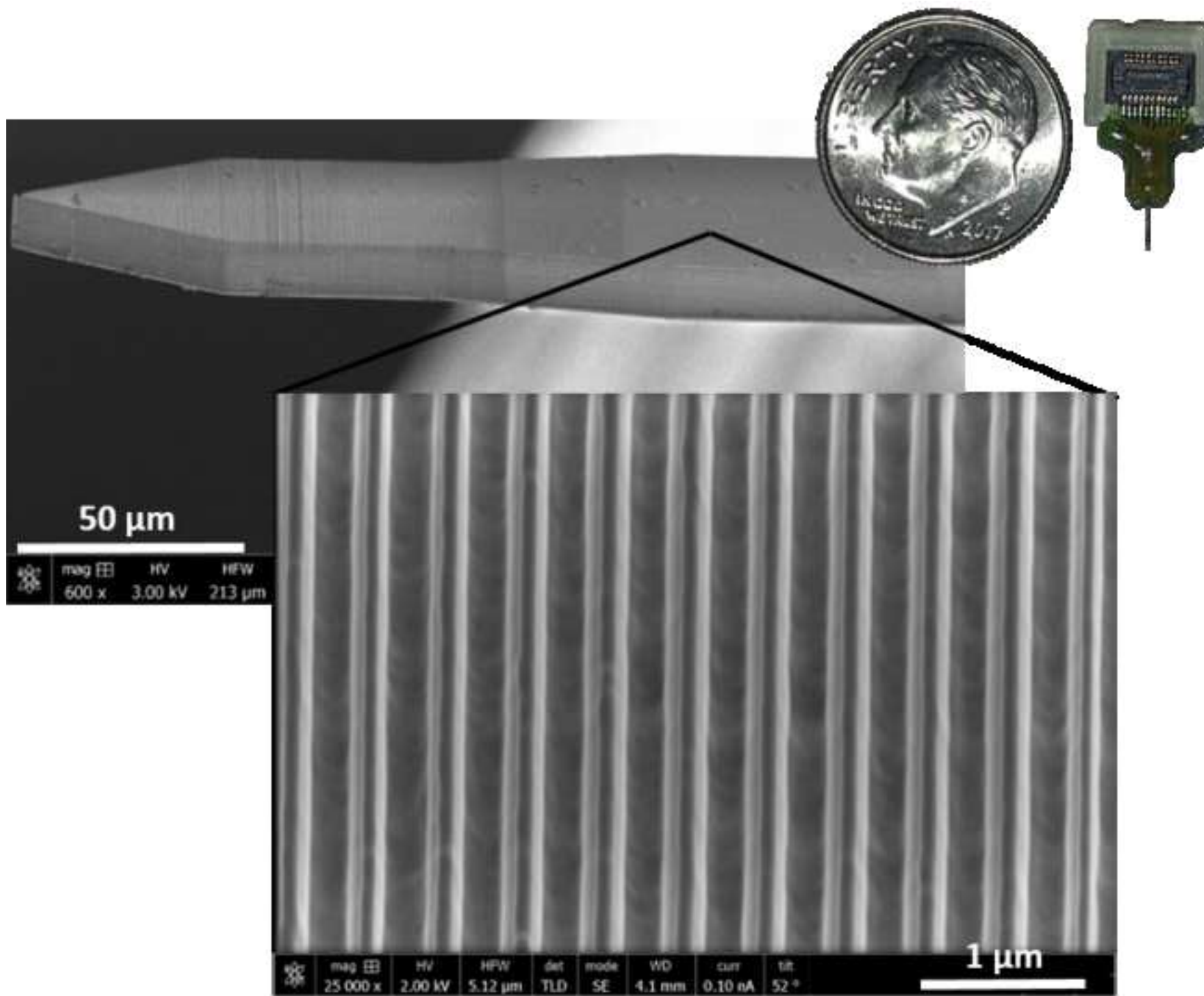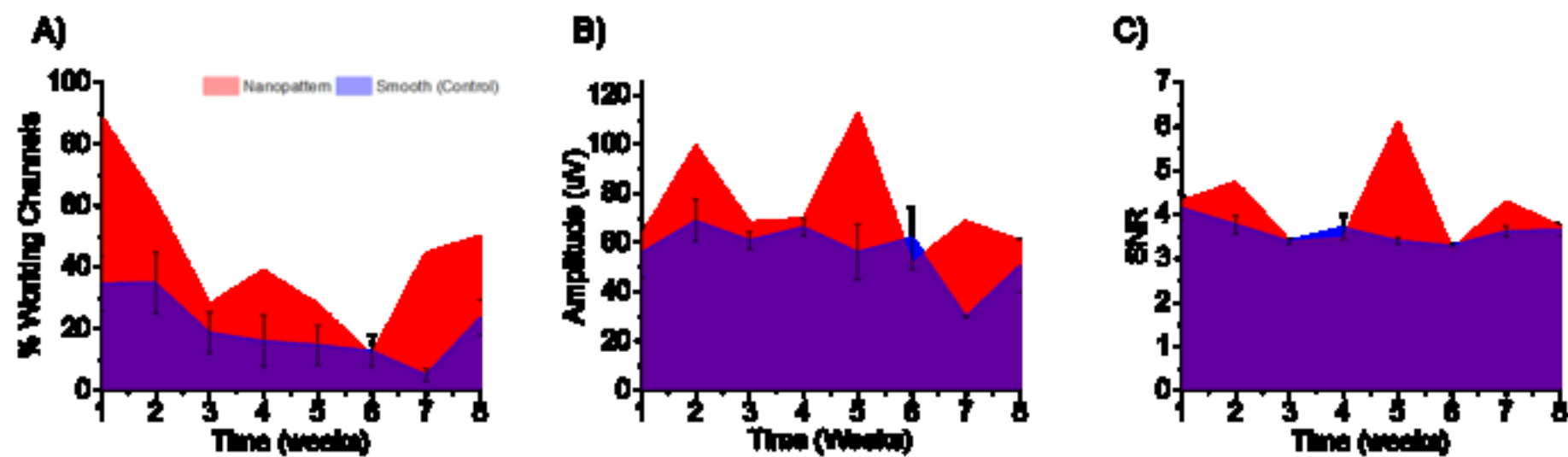834   ion beam milling: The "umbrella" method. *Ultramicroscopy.* **186** 35-41, (2018).

835

Figure1

Figure2

Click here to access/download;Figure;Fig2.tif ±

Figure3

Figure4

50 μm

mag	HV	HFW
600 x	3.00 kV	213 μm

1 μm

mag	HV	HFW	det	mode	WD	curr	tilt
25 000 x	2.00 kV	5.12 μm	TLD	SE	4.1 mm	0.10 nA	52 °

Figure5

Figure6
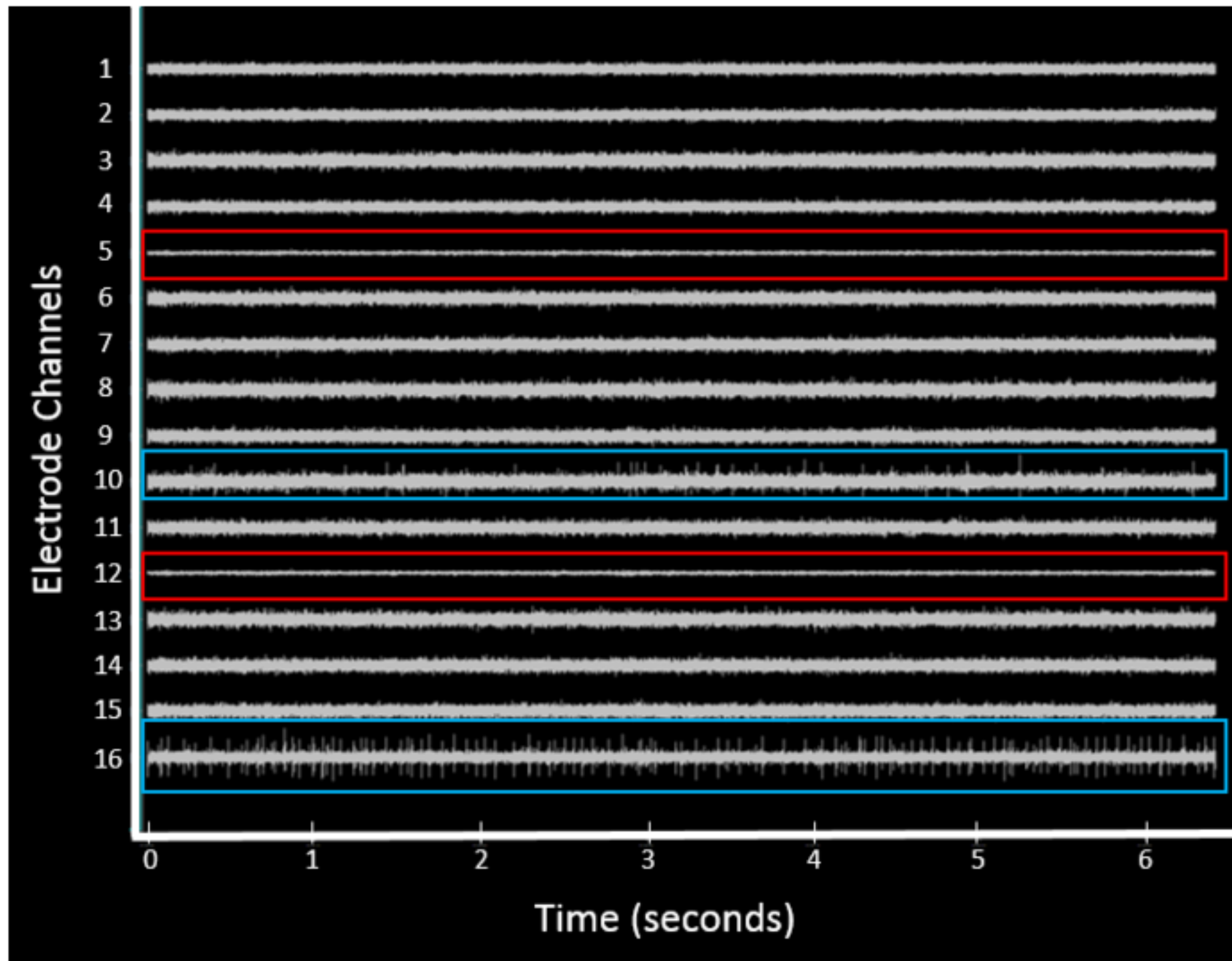
Name of Material/ Equipment	Company	Catalog Number
16-Channel ZIF-Clip Headstage	Tucker Davis Technologies	ZC16
1-meter cable, ALL spring wrapped	Thomas Scientific	1213F04
32-Channel ZIF-Clip Headstage Holder	Tucker Davis Technologies	Z-ROD32
Acetone, Thinner/Extender/Cleaner, 30ml	Ted Pella	16023
Baby-Mixter Hemostat	Fine Science Tools	13013-14
Carbon Conductive Tape, Double Coated	Ted Pella	16084-7
Corning Costar Not Treated Multiple Well Plates - 6 well	Sigma Aldrich	CLS3736-100EA
Dumont #5 Fine Forceps	Fine Science Tools	11251-30
Ethanol, 190 proof (95%), USP, Decon Labs	Fisher Scientific	22-032-600
Falcon Cell Strainer	Fisher Scientific	08-771-1
FEI, Tescan, Zeiss (also for Philips, Leo, Cambridge, Leica, CamScan), aluminum, grooved edge, Ø32mm	Ted Pella	16148
Fisherbrand Aluminum Foil, Standard-gauge roll	Fisher Scientific	01-213-101
Fisherbrand Low- and Tall-Form PTFE Evaporating Dishes	Fisher Scientific	02-617-149

Michigan-style silicon functional electrode	NeuroNexus	A1x16-3mm-100-177
Model 1772 Universal holder	KOPF	Model 1772
Model 900-U Small Animal Stereotaxic Instrument	KOPF	Model 900-U
Model 960 Electrode Manipulator with AP Slide Assembly	KOPF	Model 960
Parafilm M 10cm x 76.2m (4" x 250')	Ted Pella	807-5
PELCO Vacuum Pick-Up System, 220V	Ted Pella	520-1-220
PELCO Conductive Silver Paint	Ted Pella	16062
SEM FIB FEI Helios 650 Nanolab	Thermo Fisher Scientific	Helios G2 650

Comments/Description

The headstage and headstage holder may need to be

Any non treated petri dish will suffice

The headstage and headstage holder may need to be changed, depending on the electrode used.

Any curved hemostat will suffice.

The protocol suggested three options for mounting the functional electrode to the aluminum stub (copper or carbon conductive tape or a low profile clip. We utilized the carbon conductive tape in our study.

Any non-treated 6 well plate will suffice

Either this fine forceps or the vacuum pump will suffice

Any 95% ethanol will suffice

Depending on the SEM machine used, you may need a different size stub.

Any aluminum foil will suffice.

Any Teflon plate will suffice, this is used to dry the probes after washing on a surface they will not stick onto.

Other stereotaxic frames and accessories will suffice.

Other stereotaxic frames and accessories will suffice.

Other stereotaxic frames and accessories will suffice.

Either this vacuum pump or the fine forceps will suffice

This is the specific focused ion beam and scanning electron microscope used in the protocol. The Nanobuilder software is what it comes with. If a different FIB instrument is used, it may not be completely compatible with the protocol, specifically the steps requiring the Nanobuilder software.

Website

https://www.tdt.com/zif-clip-digital-headstages.html

https://www.thomassci.com/Laboratory-Supplies/Cell-Culture-Dishes/_/Non-Treated-Petri-Dishes?q=petri%20dish%20cell%20culture

https://www.tdt.com/zif-clip-digital-headstages.html

https://www.tedpella.com/SEMmisc_html/SEMpaint.htm#anchor16062

https://www.finescience.com/en-US/Products/Forceps-Hemostats/Hemostats/Baby-Mixter-Hemostat

https://www.tedpella.com/semmisc_html/semadhes.htm

https://www.sigmaaldrich.com/catalog/substance/corningcostarnottreatedmultiplewellplates1234598765?lang=en&region=US

https://www.finescience.com/en-US/Products/Forceps-Hemostats/Dumont-Forceps/Dumont-5-Forceps/11251-30

https://www.fishersci.com/shop/products/ethanol-190-proof-95-usp-decon-labs-10/22032600

https://www.fishersci.com/shop/products/falcon-cell-strainers-4/087711

https://www.tedpella.com/SEM_html/SEMpinmount.htm#_16180

https://www.fishersci.com/shop/products/fisherbrand-aluminum-foil-7/p-306250

https://www.fishersci.com/shop/products/fisherbrand-low-tall-form-ptfe-evaporating-dishes-12/p-88552

http://neuronexus.com/electrode-array/a1x16-3mm-100-177/

http://kopfinstruments.com/product/model-1772-universal-holder/

http://kopfinstruments.com/product/model-900-small-animal-stereotaxic-instrument1/

http://kopfinstruments.com/product/model-1772-universal-holder/

https://www.tedpella.com/grids_html/807-2.htm

http://www.tedpella.com/grids_html/Vacuum-Pick-Up-Systems.htm#anchor-520

https://www.tedpella.com/SEMmisc_html/SEMpaint.htm#anchor16062

https://www.fei.com/products/dualbeam/helios-nanolab/

jove
JOURNAL OF VISUALIZED EXPERIMENTS

1 Alewife Center #200
Cambridge, MA 02140
tel. 617.945.9051
www.jove.com

ARTICLE AND VIDEO LICENSE AGREEMENT

Title of Article:	Focused Ion Beam Lithography to Etch Nano-architectures into Microelectrodes for Improving Recording Quality and Reducing Neuroinflammation
Author(s):	Shreya Mahajan, Jonah A. Sharkins, Allen H. Hunter, Amir Avishai, Evon S. Ereifej

Item 1: The Author elects to have the Materials be made available (as described at http://www.jove.com/publish) via:

☑ Standard Access   ☐ Open Access

Item 2: Please select one of the following items:

☐ The Author is **NOT** a United States government employee.

☑ The Author is a United States government employee and the Materials were prepared in the course of his or her duties as a United States government employee.

☐ The Author is a United States government employee but the Materials were NOT prepared in the course of his or her duties as a United States government employee.

ARTICLE AND VIDEO LICENSE AGREEMENT

1.   **Defined Terms.** As used in this Article and Video License Agreement, the following terms shall have the following meanings: "**Agreement**" means this Article and Video License Agreement; "**Article**" means the article specified on the last page of this Agreement, including any associated materials such as texts, figures, tables, artwork, abstracts, or summaries contained therein; "**Author**" means the author who is a signatory to this Agreement; "**Collective Work**" means a work, such as a periodical issue, anthology or encyclopedia, in which the Materials in their entirety in unmodified form, along with a number of other contributions, constituting separate and independent works in themselves, are assembled into a collective whole; "**CRC License**" means the Creative Commons Attribution-Non Commercial-No Derivs 3.0 Unported Agreement, the terms and conditions of which can be found at: http://creativecommons.org/licenses/by-nc-nd/3.0/legalcode; "**Derivative Work**" means a work based upon the Materials or upon the Materials and other pre-existing works, such as a translation, musical arrangement, dramatization, fictionalization, motion picture version, sound recording, art reproduction, abridgment, condensation, or any other form in which the Materials may be recast, transformed, or adapted; "**Institution**" means the institution, listed on the last page of this Agreement, by which the Author was employed at the time of the creation of the Materials; "**JoVE**" means MyJove Corporation, a Massachusetts corporation and the publisher of The Journal of Visualized Experiments; "**Materials**" means the Article and / or the Video; "**Parties**" means the Author and JoVE; "**Video**" means any video(s) made by the Author, alone or in conjunction with any other parties, or by JoVE or its affiliates or agents, individually or in collaboration with the Author or any other parties, incorporating all or any portion

of the Article, and in which the Author may or may not appear.

2.   **Background.** The Author, who is the author of the Article, in order to ensure the dissemination and protection of the Article, desires to have the JoVE publish the Article and create and transmit videos based on the Article. In furtherance of such goals, the Parties desire to memorialize in this Agreement the respective rights of each Party in and to the Article and the Video.

3.   **Grant of Rights in Article.** In consideration of JoVE agreeing to publish the Article, the Author hereby grants to JoVE, subject to **Sections 4** and **7** below, the exclusive, royalty-free, perpetual (for the full term of copyright in the Article, including any extensions thereto) license (a) to publish, reproduce, distribute, display and store the Article in all forms, formats and media whether now known or hereafter developed (including without limitation in print, digital and electronic form) throughout the world, (b) to translate the Article into other languages, create adaptations, summaries or extracts of the Article or other Derivative Works (including, without limitation, the Video) or Collective Works based on all or any portion of the Article and exercise all of the rights set forth in (a) above in such translations, adaptations, summaries, extracts, Derivative Works or Collective Works and (c) to license others to do any or all of the above. The foregoing rights may be exercised in all media and formats, whether now known or hereafter devised, and include the right to make such modifications as are technically necessary to exercise the rights in other media and formats. If the "Open Access" box has been checked in **Item 1** above, JoVE and the Author hereby grant to the public all such rights in the Article as provided in, but subject to all limitations and requirements set forth in, the CRC License.

612542.6   For questions, please contact us at submissions@jove.com or +1.617.945.9051.

jove
JOURNAL OF
VISUALIZED EXPERIMENTS

1 Alewife Center #200
Cambridge, MA 02140
tel. 617.945.9051
www.jove.com

ARTICLE AND VIDEO LICENSE AGREEMENT

4.   **Retention of Rights in Article.** Notwithstanding the exclusive license granted to JoVE in **Section 3** above, the Author shall, with respect to the Article, retain the non-exclusive right to use all or part of the Article for the non-commercial purpose of giving lectures, presentations or teaching classes, and to post a copy of the Article on the Institution's website or the Author's personal website, in each case provided that a link to the Article on the JoVE website is provided and notice of JoVE's copyright in the Article is included. All non-copyright intellectual property rights in and to the Article, such as patent rights, shall remain with the Author.

5.   **Grant of Rights in Video – Standard Access.** This **Section 5** applies if the "Standard Access" box has been checked in **Item 1** above or if no box has been checked in **Item 1** above. In consideration of JoVE agreeing to produce, display or otherwise assist with the Video, the Author hereby acknowledges and agrees that, Subject to **Section 7** below, JoVE is and shall be the sole and exclusive owner of all rights of any nature, including, without limitation, all copyrights, in and to the Video. To the extent that, by law, the Author is deemed, now or at any time in the future, to have any rights of any nature in or to the Video, the Author hereby disclaims all such rights and transfers all such rights to JoVE.

6.   **Grant of Rights in Video – Open Access.** This **Section 6** applies only if the "Open Access" box has been checked in **Item 1** above. In consideration of JoVE agreeing to produce, display or otherwise assist with the Video, the Author hereby grants to JoVE, subject to **Section 7** below, the exclusive, royalty-free, perpetual (for the full term of copyright in the Article, including any extensions thereto) license (a) to publish, reproduce, distribute, display and store the Video in all forms, formats and media whether now known or hereafter developed (including without limitation in print, digital and electronic form) throughout the world, (b) to translate the Video into other languages, create adaptations, summaries or extracts of the Video or other Derivative Works or Collective Works based on all or any portion of the Video and exercise all of the rights set forth in (a) above in such translations, adaptations, summaries, extracts, Derivative Works or Collective Works and (c) to license others to do any or all of the above. The foregoing rights may be exercised in all media and formats, whether now known or hereafter devised, and include the right to make such modifications as are technically necessary to exercise the rights in other media and formats. For any Video to which this **Section 6** is applicable, JoVE and the Author hereby grant to the public all such rights in the Video as provided in, but subject to all limitations and requirements set forth in, the CRC License.

7.   **Government Employees.** If the Author is a United States government employee and the Article was prepared in the course of his or her duties as a United States government employee, as indicated in **Item 2** above, and any of the licenses or grants granted by the Author hereunder exceed the scope of the 17 U.S.C. 403, then the rights granted hereunder shall be limited to the maximum rights permitted under such statute. In such case, all provisions contained herein that are not in conflict with such statute shall remain in full force and effect, and all provisions contained herein that do so conflict shall be deemed to be amended so as to provide to JoVE the maximum rights permissible within such statute.

8.   **Protection of the Work.** The Author(s) authorize JoVE to take steps in the Author(s) name and on their behalf if JoVE believes some third party could be infringing or might infringe the copyright of either the Author's Article and/or Video.

9.   **Likeness, Privacy, Personality.** The Author hereby grants JoVE the right to use the Author's name, voice, likeness, picture, photograph, image, biography and performance in any way, commercial or otherwise, in connection with the Materials and the sale, promotion and distribution thereof. The Author hereby waives any and all rights he or she may have, relating to his or her appearance in the Video or otherwise relating to the Materials, under all applicable privacy, likeness, personality or similar laws.

10.   **Author Warranties.** The Author represents and warrants that the Article is original, that it has not been published, that the copyright interest is owned by the Author (or, if more than one author is listed at the beginning of this Agreement, by such authors collectively) and has not been assigned, licensed, or otherwise transferred to any other party. The Author represents and warrants that the author(s) listed at the top of this Agreement are the only authors of the Materials. If more than one author is listed at the top of this Agreement and if any such author has not entered into a separate Article and Video License Agreement with JoVE relating to the Materials, the Author represents and warrants that the Author has been authorized by each of the other such authors to execute this Agreement on his or her behalf and to bind him or her with respect to the terms of this Agreement as if each of them had been a party hereto as an Author. The Author warrants that the use, reproduction, distribution, public or private performance or display, and/or modification of all or any portion of the Materials does not and will not violate, infringe and/or misappropriate the patent, trademark, intellectual property or other rights of any third party. The Author represents and warrants that it has and will continue to comply with all government, institutional and other regulations, including, without limitation all institutional, laboratory, hospital, ethical, human and animal treatment, privacy, and all other rules, regulations, laws, procedures or guidelines, applicable to the Materials, and that all research involving human and animal subjects has been approved by the Author's relevant institutional review board.

11.   **JoVE Discretion.** If the Author requests the assistance of JoVE in producing the Video in the Author's facility, the Author shall ensure that the presence of JoVE employees, agents or independent contractors is in accordance with the relevant regulations of the Author's institution. If more than one author is listed at the beginning of this Agreement, JoVE may, in its sole

discretion, elect not take any action with respect to the Article until such time as it has received complete, executed Article and Video License Agreements from each such author. JoVE reserves the right, in its absolute and sole discretion and without giving any reason therefore, to accept or decline any work submitted to JoVE. JoVE and its employees, agents and independent contractors shall have full, unfettered access to the facilities of the Author or of the Author's institution as necessary to make the Video, whether actually published or not. JoVE has sole discretion as to the method of making and publishing the Materials, including, without limitation, to all decisions regarding editing, lighting, filming, timing of publication, if any, length, quality, content and the like.

12.   **Indemnification.** The Author agrees to indemnify JoVE and/or its successors and assigns from and against any and all claims, costs, and expenses, including attorney's fees, arising out of any breach of any warranty or other representations contained herein. The Author further agrees to indemnify and hold harmless JoVE from and against any and all claims, costs, and expenses, including attorney's fees, resulting from the breach by the Author of any representation or warranty contained herein or from allegations or instances of violation of intellectual property rights, damage to the Author's or the Author's institution's facilities, fraud, libel, defamation, research, equipment, experiments, property damage, personal injury, violations of institutional, laboratory, hospital, ethical, human and animal treatment, privacy or other rules, regulations, laws, procedures or guidelines, liabilities and other losses or damages related in any way to the submission of work to JoVE, making of videos by JoVE, or publication in JoVE or elsewhere by JoVE. The Author shall be responsible for, and shall hold JoVE harmless from, damages caused by lack of sterilization, lack of cleanliness or by contamination due to

the making of a video by JoVE its employees, agents or independent contractors. All sterilization, cleanliness or decontamination procedures shall be solely the responsibility of the Author and shall be undertaken at the Author's expense. All indemnifications provided herein shall include JoVE's attorney's fees and costs related to said losses or damages. Such indemnification and holding harmless shall include such losses or damages incurred by, or in connection with, acts or omissions of JoVE, its employees, agents or independent contractors.

13.   **Fees.** To cover the cost incurred for publication, JoVE must receive payment before production and publication of the Materials. Payment is due in 21 days of invoice. Should the Materials not be published due to an editorial or production decision, these funds will be returned to the Author. Withdrawal by the Author of any submitted Materials after final peer review approval will result in a US$1,200 fee to cover pre-production expenses incurred by JoVE. If payment is not received by the completion of filming, production and publication of the Materials will be suspended until payment is received.

14.   **Transfer, Governing Law.** This Agreement may be assigned by JoVE and shall inure to the benefits of any of JoVE's successors and assignees. This Agreement shall be governed and construed by the internal laws of the Commonwealth of Massachusetts without giving effect to any conflict of law provision thereunder. This Agreement may be executed in counterparts, each of which shall be deemed an original, but all of which together shall be deemed to me one and the same agreement. A signed copy of this Agreement delivered by facsimile, e-mail or other means of electronic transmission shall be deemed to have the same legal effect as delivery of an original signed copy of this Agreement.

A signed copy of this document must be sent with all new submissions. Only one Agreement is required per submission.

CORRESPONDING AUTHOR

Name:

Evon S. Ereifej, Ph.D.

Department:

Rehabilitation Research and Developement / Departments of Neurology and Biomedical Engineering
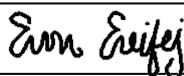
Institution:

Veteran Affairs Medical Center / University of Michigan

Title:

Research Investigator

Signature:

Evon Ereifej

Date:

March 15, 2019

Please submit a **signed** and **dated** copy of this license by one of the following three methods:

1. Upload an electronic version on the JoVE submission site
2. Fax the document to +1.866.381.2236
3. Mail the document to JoVE / Attn: JoVE Editorial / 1 Alewife Center #200 / Cambridge, MA 02140

VA Ann Arbor Healthcare System
2215 Fuller Road
Ann Arbor, MI 48105

Dr. Evon S. Ereifej
Research Investigator

Veteran Affairs Medical Center
Department of Neurology
Department of Biomedical Engineering
University of Michigan
2215 Fuller Rd
Ann Arbor, MI 48105

E-mail eereifej@umich.edu

Vineeta Bajaj, Ph.D.
Review Editor, JoVE

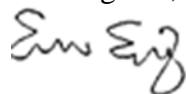May 30, 2019

Resubmission Invited Manuscript

Dear Dr. Bajaj and Editorial Board:

We thank you for the further careful examination of our manuscript entitled "**Focused Ion Beam Lithography to Etch Nano-architectures into Microelectrodes**" by Shreya Mahajan, Jonah A. Sharkins, Allen H. Hunter, Amir Avishai, and myself, for consideration for publication in the Journal of Visualized Experiments (JoVE).

Please find below our detailed reply to the editors, with point-by-point responses and references to changes in the manuscript. For your convenience, the editor's comments are copied in bolded font, and changes to the revised text were incorporated by track changes throughout for your ease of finding the changes.

Please contact us if there is anything we can do to help make your final decision a favorable one. Thank you for the opportunity to contribute to this exciting body of work!

Best regards,

Evon S. Ereifej, Ph.D.

Editorial comments:

1. The protocol section doesn't show how this is done. The title should be in alignment with the protocol being presented. Please remove these words from the title.

The title has been modified to remove "for Improving Recording Quality and Reducing Neuroinflammation".

2. The length of the protocol section cannot be more than 10 pages including headings and spacing. Presently the protocol is around 11 pages. Please combine shorter protocol steps so that individual steps contain only 2-3 actions per step.

We have combined shorter protocol steps/sub-steps together to ensure that the protocol is no more than 10 pages (currently it is ~7 pages).

3. The hard-cut limit for the highlighted section is than 2.75 pages including headings and spacings. Presently this is around 6 pages. Please adjust the highlights accordingly. Also, if a substep is highlighted, the step/heading associated with it needs to be highlighted as well. So maybe consider removing some of the subheadings and consider combining shorter protocol step so there are 2-3 actions per step and no more than 4 sentences per step.

We have taken all of the advice from the editor to ensure that the highlighted section of the protocol meets the 2.75 page limit.

4. We cannot have more than one note following a step or a sub step. Moved here instead. Please check.

The new placement of the note makes sense, thank you.

5. Some of the details can be moved to the discussion section.

We took the editor's advice and removed this note from the protocol section and ensured that the information is in the discussion section instead.

6. Please include a note stating what is the significance of home staging.

We included a note stating that the importance of home staging is, "Running the home stage operation is a preventative step to ensure the stage axis are read correctly by the software and the microscope is in good condition."

7. Notes cannot be filmed so highlights are removed.

Thank you for this tip, we removed the highlights from all notes in the "to be filmed" sections.

8. We cannot have commercial terms in the manuscript. Please use generic term instead. Please move the commercial term to the Table of Materials and refer to the table wherever needed.

We replaced the term "Nav-Cam" with "navigation camera". The Nav-cam is an optical camera mounted on the microscope that is used to assist with sample navigation, especially when you have more than one sample in the chamber. The term Nav-Cam is probably specific to FEI/ThermoFisher, but there are similar devices on other microscope brands, so replacing with a generic term will be suitable for the protocol.

9. So this is "xT Align Feature" the inbuilt command?

Yes, the xT align feature is built in to the software. It exists on all FEI microscopes made in the last 15 years or so. We added the phrase "built in" before the "xT Align Feature" in the protocol to note that.

10. We cannot have commercial terms in the manuscript. Please move this to the table of materials and use generic term instead. Please refer to the table of materials wherever applicable.

We replaced all reference to "Nanobuilder software" to simply "software", "FEI microscope" to "SEM microscope", "Michigan-style silicon microelectrodes" to "single shank silicon microelectrodes" and removed all model and product numbers from within the protocol.

RightsLink®

Copyright Clearance Center

Home   Create Account   Help

Title: The Neuroinflammatory Response to Nanopatterning Parallel Grooves into the Surface Structure of Intracortical Microelectrodes

Author: Evon S. Ereifej, Cara S. Smith, Seth M. Meade, et al

Publication: Advanced Functional Materials

Publisher: John Wiley and Sons

Date: Dec 4, 2017

© WILEY-VCH Verlag GmbH & Co. KGaA, Weinheim

Quick Price Estimate

Please review the credit line for the requested figure/table.
If the figure/table you wish to reproduce is credited to a source other than the author of the publication (i.e third party material) you will need to obtain permission from that copyright holder, book or journal before making any use of the material. For the avoidance of doubt – any and all third party content is expressly excluded from this permission.
Otherwise please proceed with your order.

John Wiley and Sons grants a license for all orders, including $0 orders. Please select the Continue button and place an order for this reuse.

As the Author of this content you retain the right to re-use the final version (or parts thereof) in any new publication you are authoring, co-authoring or editing (excluding journal articles) where the re-used material constitutes less than half of the total material in the publication. In such case, any modifications should be accurately noted.
If you still require a license, please proceed with your order. You will not be charged for this permission.

I would like to...	reuse in a journal/magazine ▼
Requestor Type	Author of this Wiley article ▼
Is the reuse sponsored by or associated with a pharmaceutical or medical products company?	No ▼
Format	Print and electronic ▼
Portion	Figure/table ▼
Number of figures/tables	3
Will you be translating?	No ▼
Circulation	10000
Select your currency	USD - $ ▼
Quick Price	0.00 USD

Content Delivery: A copy of this content may be purchased following completion of your permissions order. High Res Image files - please contact Wiley

QUICK PRICE   CONTINUE

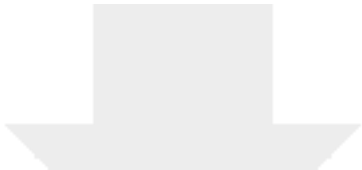Information regarding permissions for developing countries.
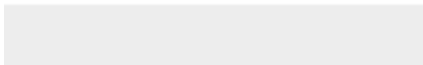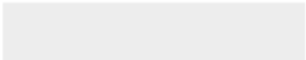
Click here to access/download
Supplemental Coding Files
Case Western 2000 micron Final 11H47M runtime
(1).nbj

Figure 1 High Res

Click here to access/download
Supplemental Coding Files
Fig1EWM (1).emf

Figure 2 High Res

Click here to access/download
Supplemental Coding Files
Fig2EWM.emf

Figure 3 High Res

Click here to access/download
Supplemental Coding Files
Fig3EWM.emf

Figure 4 High Res

Click here to access/download
Supplemental Coding Files
Fig4EWM.emf

Figure 5 High Res

Click here to access/download
Supplemental Coding Files
Fig5EWM.emf

Figure 6 High Res

Click here to access/download
Supplemental Coding Files
Fig6EWM.emf